

Low-Rank Structured MMSE Channel Estimation with Mixtures of Factor Analyzers

Benedikt Fesl, Nurettin Turan, and Wolfgang Utschick

School of Computation, Information and Technology, Technical University of Munich, Germany

Email: {benedikt.fesl, nurettin.turan, utschick}@tum.de

Abstract—This work proposes a generative modeling-aided channel estimator based on mixtures of factor analyzers (MFA). In an offline step, the parameters of the generative model are inferred via an expectation-maximization (EM) algorithm in order to learn the underlying channel distribution of a whole communication scenario inside a base station (BS) cell. Thereby, the wireless channels are effectively modeled on a piecewise linear subspace which is achieved by the low-rank structure of the learned covariances of the MFA. This suits the low-rank structure of wireless channels at high frequencies and additionally saves parameters and prevents overfitting. Afterwards, the trained MFA model is used online to perform channel estimation with a closed-form solution of the estimator which asymptotically converges to the minimum mean square error (MMSE) estimator. Numerical results based on real-world measurements demonstrate the great potential of the proposed approach for channel estimation.

Index Terms—Mixtures of factor analyzers, channel estimation, low-complexity, variational inference, machine learning.

I. INTRODUCTION

The concept of generative models has been existing for a long time. [1]. One prominent example is the Gaussian mixture model (GMM), which has the ability for universal approximation [2]. With the advent of deep learning, generative models based on neural networks, such as variational autoencoders (VAEs) [3], have become highly successful. Therefore, generative models play a key role in modern signal processing and wireless communication applications, particularly when domain and system knowledge is incorporated to solve inference tasks [4]. In this respect, the requirements for accurate channel estimation in the next generation of cellular systems (6G) are of significant interest [5].

In recent works, both GMMs and VAEs were leveraged to learn the underlying channel distribution of a whole communication scenario and to utilize this information to yield a tractable prior information for channel estimation, showing great improvements over state-of-the-art approaches [6], [7]. The advantages are the possibilities to incorporate structural features and even learn from imperfect data [8], [9]. A key feature of both approaches is the parameterization of the local distribution of the mobile terminals (MTs) inside a BS cell in a tractable manner by the learned parameters. This allows to utilize closed-form solutions for the estimation task.

Although these methods show promising results, they face some challenges which can potentially hinder the application

in real systems. First, the number of learned parameters is high, entailing demanding memory requirements. For instance, the number of parameters scales quadratically in the number of antennas for the GMM; Likewise, the VAE is comprised of deep neural networks (NNs) with typically even more parameters. While structural features imposed by antenna arrays can reduce the number of parameters, mutual coupling between the antennas or other hardware imperfections can corrupt this structure in real systems. Second, the generative abilities of GMMs are known to be somewhat limited due to the discrete nature of the latent space, whereas VAEs are generally lacking interpretability due to the elaborate design of nested nonlinearities.

A powerful generative model that is related to GMMs and VAEs is the MFA model, which contains both a discrete and continuous latent variable, where the latter is modeled Gaussian just as in the VAE [10, Ch. 12], [11]. This motivated the usage of MFA for several applications, e.g. [12], [13]. In contrast to the VAE with a nonlinear latent space, the latent space of the MFA is piecewise linear with tractable expressions for the inference of the latent samples. From a different perspective, the MFA model can be interpreted as a GMM with low-rank structured covariances [10, Ch. 12]. This results in having less parameters and being less prone to overfitting, thereby matching the structural features of channels at high frequencies [14]. Altogether, the MFA model has the potential to excellently match the requirements for accurate channel estimation in 6G systems with low overhead.

Contributions: We propose to employ the MFA model to learn the unknown underlying channel distribution of a whole BS cell with low-rank structured covariances which effectively models the channel distribution on a piecewise linear subspace. The resulting channel estimator can be computed in closed form by a convex combination of linear MMSE (LMMSE) estimates, which asymptotically converges to the generally intractable mean square error (MSE)-optimal solution. We validate the effectiveness of the approach through simulation results based on real-world measurement data, which demonstrate that the MFA achieve great results in channel estimation performance.

II. SYSTEM MODEL AND MEASUREMENT CAMPAIGN

We consider a single-input multiple-output (SIMO) communication scenario where the BS equipped with N antennas receives uplink training signals from a single-antenna MT. In

The authors acknowledge the financial support by the Federal Ministry of Education and Research of Germany in the program of “Souverän. Digital. Vernetzt.”. Joint project 6G-life, project identification number: 16KISK002.

particular, at the BS, after decorrelating the pilot signal, noisy observations of the form

$$\mathbf{y} = \mathbf{h} + \mathbf{n} \in \mathbb{C}^N \quad (1)$$

are received where the channel $\mathbf{h} \in \mathbb{C}^N$, which follows an unknown distribution $p(\mathbf{h})$, is corrupted by additive white Gaussian noise (AWGN) $\mathbf{n} \sim \mathcal{N}_{\mathbb{C}}(\mathbf{0}, \sigma^2 \mathbf{I})$. Although the underlying channel distribution $p(\mathbf{h})$ is unknown, we assume the availability of a training dataset $\mathcal{H} = \{\mathbf{h}_t\}_{t=1}^T$ of T channel samples that represent the channel distribution of the whole BS cell. A common practice is to use simulation tools which are based on sophisticated models of the underlying communication scenario to generate a dataset, however, these models do not fully capture the characteristics of the real world. Therefore, we use real-world data from a measurement campaign which is described in the following.

The measurement campaign was conducted at the Nokia campus in Stuttgart, Germany, in October/November 2017. As can be seen in Fig. 1, the receive antenna with a down-tilt of 10° was mounted on a rooftop about 20 m above the ground and comprises a uniform rectangular array (URA) with $N_v = 4$ vertical and $N_h = 16$ horizontal single polarized patch antennas. The horizontal spacing is $\lambda/2$ and the vertical spacing equals λ , where the geometry of the BS antenna array was adapted to the urban microcell (UMi) propagation scenario. The carrier frequency is 2.18 GHz. The BS transmitted time-frequency orthogonal pilots using 10 MHz orthogonal frequency-division multiplexing (OFDM) waveforms. In particular, 600 subcarriers with 15 kHz spacing were used, which resembles typical Long Term Evolution (LTE) numerology. The pilots were sent continuously with a periodicity of 0.5 ms and were arranged in 50 separate subbands, with 12 consecutive subcarriers each, for channel sounding purposes. For the duration of one pilot burst the propagation channel was assumed to remain constant. A single monopole receive antenna, which mimics the MT, was mounted on top of a moving vehicle at a height of 1.5 m. The maximum speed was 25 kmph. Synchronization between the transmitter and receiver was achieved using GPS. The data was collected by a TSMW receiver and stored on a Rohde & Schwarz IQR hard disk recorder. In a post-processing step, by the correlation of the received signal with the pilot sequence a channel realization vector with $N = N_v N_h$ coefficients per subband was extracted.

The measurement was conducted at a high signal-to-noise ratio (SNR), which ranged from 20 dB to 30 dB. Thus, the measured channels are regarded as ground truth. In this work, we will therefore consider a system where we artificially corrupt the measured channels with AWGN at specific SNRs and thereby obtain noisy observations $\mathbf{y} = \mathbf{h} + \mathbf{n}$. We note that we investigate a single-snapshot scenario, i.e., the coherence interval of the covariance matrix and of the channel is identical.

III. MIXTURE OF FACTOR ANALYZERS

We start by briefly revising the factor analysis (FA) which is the basis for the MFA. The generative model is given as

$$\mathbf{h}^{(L)} = \mathbf{W}\mathbf{z} + \mathbf{u} \quad (2)$$

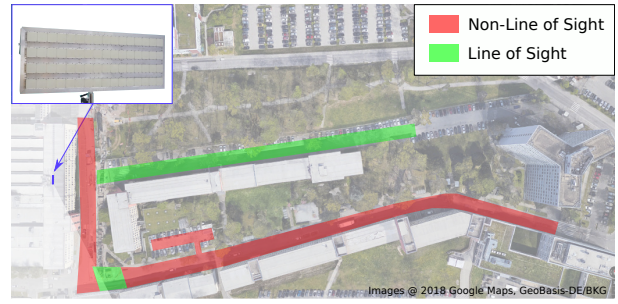


Fig. 1: Measurement setup on the Nokia campus in Stuttgart, Germany.

where $\mathbf{W} \in \mathbb{C}^{N \times L}$ is the so called factor loading matrix, $\mathbf{z} \in \mathbb{C}^L$ is the latent variable, and $\mathbf{u} \sim \mathcal{N}_{\mathbb{C}}(\mathbf{0}, \Psi)$ is an additive term. The prior distribution is assumed to be standard Gaussian, i.e., $p(\mathbf{z}) = \mathcal{N}_{\mathbb{C}}(\mathbf{z}; \mathbf{0}, \mathbf{I})$. The key assumptions for this model are that the latent variable \mathbf{z} is low-dimensional, i.e., $L < N$ holds, and that the covariance Ψ is diagonal. The rationale is that the data are modeled on a linear subspace described by \mathbf{W} , which explains the common factors/features and their correlations, and the additional term \mathbf{u} accounts for both unique factors and noise in the data [10, Ch. 12]. Note that if $\Psi = \psi^2 \mathbf{I}$ or $\Psi = \mathbf{0}$, the FA degenerates to the (probabilistic) principle component analysis (PCA). Moreover, the FA is a low-rank parameterization of a Gaussian, i.e., $\mathbf{h}^{(L)} \sim \mathcal{N}_{\mathbb{C}}(\mathbf{0}, \mathbf{W}\mathbf{W}^H + \Psi)$, cf. [10, Ch. 12].

Since the linearity of the latent space and the Gaussian assumption of the data is too restrictive for modeling real-world communication scenarios, we aim for a more powerful generative model which is realized by the MFA. Thereby, a mixture of K linear subspaces is considered which yields the following generative model for the k th mixture component:

$$\mathbf{h}^{(K,L)} | k = \mathbf{W}_k \mathbf{z} + \mathbf{u}_k + \boldsymbol{\mu}_k \quad (3)$$

where $\mathbf{W}_k \in \mathbb{C}^{N \times L}$ is the factor loading matrix of mixture k , $\mathbf{u}_k \sim \mathcal{N}_{\mathbb{C}}(\mathbf{0}, \Psi_k)$, and $\boldsymbol{\mu}_k$ is the mean of mixture k . The resulting generative model then follows the distribution

$$p^{(K,L)}(\mathbf{h}) = \sum_{k=1}^K \int p(\mathbf{h} | \mathbf{z}, k) p(\mathbf{z} | k) p(k) d\mathbf{z} \quad (4)$$

where $p(\mathbf{z}|k) = p(\mathbf{z}) = \mathcal{N}_{\mathbb{C}}(\mathbf{0}, \mathbf{I})$ and $p(k)$ follows a categorical distribution [10, Ch. 12]. An important property for our considerations is that, given the latent variables, the distribution is conditionally Gaussian, i.e.,

$$p^{(K,L)}(\mathbf{h} | \mathbf{z}, k) = \mathcal{N}_{\mathbb{C}}(\mathbf{h}; \boldsymbol{\mu}_k + \mathbf{W}_k \mathbf{z}, \Psi_k). \quad (5)$$

By integrating out the latent variable \mathbf{z} in (4), one can interpret the MFA as a GMM with low-rank structured covariances, i.e.,

$$p^{(K,L)}(\mathbf{h}) = \sum_{k=1}^K p(k) \mathcal{N}_{\mathbb{C}}(\mathbf{h}; \boldsymbol{\mu}_k, \mathbf{W}_k \mathbf{W}_k^H + \Psi_k). \quad (6)$$

This model has generally much less parameters than a GMM with full covariances since $L < N$. Note that there exist different restrictions on the diagonal covariance matrix Ψ_k , e.g., it is possible to choose a common matrix for all components

as $\Psi_k = \Psi$, $\forall k \in \{1, \dots, K\}$, or to choose a scaled identity $\Psi_k = \psi_k^2 \mathbf{I}$, yielding different degrees of freedom.

Given a training dataset \mathcal{H} , an EM algorithm can be used to fit the parameters of the MFA model [11]. Interestingly, the MFA model meets all formal requirements for the universal approximation property from [2] in the sense that, for an infinite number of mixture components, any continuous probability density function (PDF) can be asymptotically approximated arbitrarily well by means of MFA as

$$\lim_{K \rightarrow \infty} \|p(\mathbf{h}) - p^{(K,L)}(\mathbf{h})\|_\infty = 0. \quad (7)$$

It is worth noting that this result holds for an any number L of latent dimensions which is a powerful basis for our consideration of learning a tractable approximation of the underlying channel distribution by means of the MFA. In view of this property, in this work we investigate the asymptotic behavior of the MFA-based channel estimator and the relationship between the number of latent dimensions L and the number of mixture components K for a given number of training samples T .

IV. CHANNEL ESTIMATION

In this section, we derive an approximation of the generally intractable MMSE estimator via the MFA model. The MSE-optimal estimator for an arbitrary channel distribution is the conditional mean estimator (CME) which is given as

$$\hat{\mathbf{h}}_{\text{CME}}(\mathbf{y}) = \mathbb{E}[\mathbf{h} \mid \mathbf{y}] = \int \mathbf{h} p(\mathbf{h} \mid \mathbf{y}) d\mathbf{h}. \quad (8)$$

Note that this estimator cannot be computed generally since the conditional distribution $p(\mathbf{h} \mid \mathbf{y})$ is unknown. Even if the channel distribution $p(\mathbf{h})$ would be known, computing the CME via the integral is intractable in real-time systems. To this end, one needs tractable expressions of the involved distributions such that the resulting estimator can be computed with a manageable complexity.

A. MFA-based Channel Estimator

We aim to find a tractable expression of the CME by using the learned MFA model and introduce the discrete latent variable via the law of total expectation:

$$\hat{\mathbf{h}}^{(K,L)}(\mathbf{y}) = \mathbb{E}[\mathbf{h}^{(K,L)} \mid \mathbf{y}] = \mathbb{E} \left[\mathbb{E}[\mathbf{h}^{(K,L)} \mid \mathbf{y}, k] \mid \mathbf{y} \right]. \quad (9)$$

We note that, since conditioned on the component k the model is Gaussian, i.e., $\mathbf{h}^{(K,L)} \mid k \sim \mathcal{N}_{\mathbb{C}}(\boldsymbol{\mu}_k, \mathbf{W}_k \mathbf{W}_k^H + \Psi_k)$, cf. (6), we can use the well-known LMMSE formula to solve the inner expectation in closed form, which yields

$$\mathbb{E}[\mathbf{h}^{(K,L)} \mid \mathbf{y}, k] = \boldsymbol{\mu}_k + (\mathbf{W}_k \mathbf{W}_k^H + \Psi_k) (\mathbf{W}_k \mathbf{W}_k^H + \Psi_k + \sigma^2 \mathbf{I})^{-1} (\mathbf{y} - \boldsymbol{\mu}_k). \quad (10)$$

The outer expectation in (9) is then, due to the discrete nature of the latent variable, a convex combination of the linear filters from (10), given as

$$\hat{\mathbf{h}}^{(K,L)}(\mathbf{y}) = \sum_{k=1}^K p(k \mid \mathbf{y}) \mathbb{E}[\mathbf{h}^{(K,L)} \mid \mathbf{y}, k] \quad (11)$$

where $p(k \mid \mathbf{y})$ is the responsibility of the k th component for the pilot observation \mathbf{y} which is computed as

$$p(k \mid \mathbf{y}) = \frac{p(k) \mathcal{N}_{\mathbb{C}}(\mathbf{y}; \boldsymbol{\mu}_k, \mathbf{W}_k \mathbf{W}_k^H + \Psi_k + \sigma^2 \mathbf{I})}{\sum_{i=1}^K p(i) \mathcal{N}_{\mathbb{C}}(\mathbf{y}; \boldsymbol{\mu}_i, \mathbf{W}_i \mathbf{W}_i^H + \Psi_i + \sigma^2 \mathbf{I})}. \quad (12)$$

In the next subsections, we investigate the asymptotic behavior of the estimator for an increasing number of mixture components and discuss the complexity and memory requirements of the estimator based on the low-rank structure.

B. Asymptotic Optimality

In [6, Theorem 2], it is shown that the CME approximation via an estimator based on a GMM which is learned on the underlying channel distribution is asymptotically converging to the true CME for large numbers K of mixture components. The key prerequisite for this result is the convergence of the approximate distribution to the true channel distribution as a consequence of the universal approximation property of the GMM. Due to space limitations we do not restate [6, Theorem 2] in this work. Building on this result, we can state the asymptotic optimality of the MFA-based channel estimator (11) as a direct consequence of [6, Theorem 2] by using the universal approximation property.

Corollary 1. *Let $p(\mathbf{h})$ be any continuous PDF which vanishes at infinity. For an arbitrary number of latent dimensions L , the MFA-based channel estimator (11) converges to the true MSE-optimal CME (8) in the sense that*

$$\lim_{K \rightarrow \infty} \|\hat{\mathbf{h}}_{\text{CME}}(\mathbf{y}) - \hat{\mathbf{h}}^{(K,L)}(\mathbf{y})\| = 0 \quad (13)$$

holds for any given \mathbf{y} .

Proof. The result is a direct consequence of [6, Theorem 2] by using the universal approximation ability (7) of the MFA model which follows from [2, Theorem 5]. \square

Corollary 1 shows the powerful abilities of the MFA-based channel estimator in combination with the possibility to reduce the latent dimension L . That said, the practicability of the estimator for a fixed number L of latent dimensions and a finite number K of mixtures is yet to be investigated. We will therefore show simulation results that demonstrate the strong performance of the estimator for real-world data for different numbers of mixtures and latent dimensions in Section V.

C. Baseline Channel Estimators

We first discuss non-data-based channel estimators, one of whom is the least squares (LS) estimator which simply computes $\hat{\mathbf{h}}_{\text{LS}} = \mathbf{y}$ in our case. Another technique is compressive sensing, where the channel is assumed to be (approximately) sparse such that we have $\mathbf{h} \approx \boldsymbol{\Delta} \mathbf{s}$ for a sparse vector $\mathbf{s} \in \mathbb{C}^M$. The dictionary $\boldsymbol{\Delta} \in \mathbb{C}^{N \times M}$ is typically an oversampled discrete Fourier transform (DFT) matrix [15]. A baseline algorithm is orthogonal matching pursuit (OMP) [16] which recovers an estimate $\hat{\mathbf{s}}$ of \mathbf{s} assuming $\mathbf{y} = \boldsymbol{\Delta} \mathbf{s} + \mathbf{n}$ and estimates the channel as $\hat{\mathbf{h}}_{\text{OMP}} = \boldsymbol{\Delta} \hat{\mathbf{s}}$ for which OMP needs to know the sparsity order. Since order estimation is a difficult

Name	Parameters	$L = 2$	$L = 8$	$L = 16$
MFA	$K(LN + N + 2)$	$1.24 \cdot 10^4$	$3.67 \cdot 10^4$	$6.98 \cdot 10^4$
GMM full	$K(\frac{1}{2}N^2 + 2N + 1)$		$1.39 \cdot 10^5$	
GMM toep	$K(5N + 1)$		$2.05 \cdot 10^4$	
GMM circ	$K(2N + 1)$		$8.26 \cdot 10^3$	

TABLE I: Analysis of the number of parameters of the MFA model as compared to a (structured) GMM with example numbers for $K = N = 64$.

problem, we use a genie-aided approach: OMP gets access to the true channel to choose the optimal sparsity. We employ the OMP algorithm with $M = 4N$.

Next, we investigate state-of-the-art data-based algorithms. An important baseline is the LMMSE formula based on the sample covariance matrix. For this, we use all T training data from \mathcal{H} to compute $\mathbf{C} = \frac{1}{T} \sum_{t=1}^T \mathbf{h}_t \mathbf{h}_t^H$ and then estimate channels as $\hat{\mathbf{h}}_{\text{LMMSE}} = \mathbf{C}(\mathbf{C} + \sigma^2 \mathbf{I})^{-1} \mathbf{y}$. A convolutional neural network (CNN)-based channel estimator was introduced in [17] whose architecture is derived via insights about the channel/system model. The activation function is the rectified linear unit (ReLU) and we use the $2N \times N$ truncated DFT matrix as input transform, cf. [17, eq. (43)]. Thereby, an independent CNN is trained for each SNR value. A related technique to the proposed MFA approach is the GMM-based channel estimator from [6], [8] which learns a GMM of the form $p^{(K)}(\mathbf{h}) = \sum_{k=1}^K p(k) \mathcal{N}_{\mathbf{C}}(\mathbf{h}; \boldsymbol{\mu}_k, \mathbf{C}_k)$ via an EM algorithm to approximate the underlying channel distribution with generally full covariances \mathbf{C}_k . In [8], the case of circulant and Toeplitz structured covariances is discussed where the underlying EM algorithm is adapted to have covariances of the form $\mathbf{C}_k = \mathbf{Q}^H \text{diag}(c_k) \mathbf{Q}$ where \mathbf{Q} is a (truncated) DFT matrix for the (Toeplitz) circulant case. The resulting estimator then is of the form

$$\hat{\mathbf{h}}_{\text{GMM}} = \sum_{k=1}^K p(k | \mathbf{y}) \left(\boldsymbol{\mu}_k + \mathbf{C}_k \mathbf{C}_{\mathbf{y},k}^{-1} (\mathbf{y} - \boldsymbol{\mu}_k) \right) \quad (14)$$

where $\mathbf{C}_{\mathbf{y},k} = \mathbf{C}_k + \sigma^2 \mathbf{I}$ and $p(k | \mathbf{y})$ is the responsibility of component k for pilot \mathbf{y} , cf. [6], [8]. In [18], the GMM-based estimator was already evaluated on measurement data.

D. Memory and Complexity Analysis

In this subsection, we analyze the memory requirements and the computational (online) complexity of the MFA-based channel estimator. We emphasize that the fitting of the parameters via the EM algorithm is done exclusively in an initial offline phase. In the online phase, the channel estimate in (11) is computed for a given pilot observation \mathbf{y} . We first note that the calculation of the K LMMSE filters in (10) as well as of the K responsibilities in (12) can be parallelized which is of great importance in real-time systems. Furthermore, due to the specific structure of the parameterized covariances, the inverse that appears in (10) and in (12)—for evaluating

the Gaussian density—can be computed less expensively by means of the inversion lemma as

$$(\mathbf{W}_k \mathbf{W}_k^H + \boldsymbol{\Psi}_k + \sigma^2 \mathbf{I})^{-1} = \mathbf{D}_k - \mathbf{D}_k \mathbf{W}_k \mathbf{A}_k \mathbf{W}_k^H \mathbf{D}_k \quad (15)$$

where $\mathbf{D}_k = (\boldsymbol{\Psi}_k + \sigma^2 \mathbf{I})^{-1}$ is a diagonal matrix and $\mathbf{A}_k = (\mathbf{I} + \mathbf{W}_k^H \mathbf{D}_k \mathbf{W}_k)^{-1}$ is an $L \times L$ matrix of lower dimension. Thus, the overall order of complexity of the channel estimator is $\mathcal{O}(K(N^2 + NL^2))$ when taking the computation of the matrix products into account. However, since the LMMSE filters are fixed for a given SNR value, they can be pre-computed such that only matrix-vector products have to be evaluated. In this case, the complexity reduces to $\mathcal{O}(KN^2)$ which can be computed in K parallel processes.

The memory requirement is determined by the number of parameters for $\{\mathbf{W}_k, \boldsymbol{\Psi}_k, \boldsymbol{\mu}_k, p(k)\}_{k=1}^K$, which depends on the choice of the diagonal covariances $\boldsymbol{\Psi}_k$. As discussed also later, the option of having scaled identities $\boldsymbol{\Psi}_k = \psi_k^2 \mathbf{I}$, $\forall k \in \{1, \dots, K\}$ saves memory overhead and does not affect the channel estimation performance. In this case, the total number of parameters is $K(LN + N + 2)$. In Table I, we compare the number of parameters with the related GMM estimator from [6], [8] where we exemplarily depict the number of parameters for a setting with $K = N = 64$ for different numbers L of latent dimensions. This particular setting is evaluated in Section V in terms of the channel estimation performance. In comparison to the GMM estimator with full covariances, the number of parameters is drastically reduced, which is beneficial against overfitting as shown later. Although the GMM with structured covariances can have an even lower number of parameters, the performance in this case might suffer from too restrictive assumptions on the underlying structure which is also verified by the simulation results. Altogether, the MFA model allows for an adaptivity in the number of parameters which reflects a trade-off between memory overhead, computational complexity, and estimation performance which can be conveniently optimized for a certain application scenario.

V. SIMULATION RESULTS

We conducted numerical experiments for the data from the measurement campaign as discussed in Section II with $N = 64$ antennas. The channels are normalized such that $\mathbb{E}[\|\mathbf{h}\|_2^2] = N$, and the SNR is defined as $1/\sigma^2$. The MSE between the true and estimated channels is normalized by N . For the MFA model we restrict the covariances to $\boldsymbol{\Psi}_k = \psi_k^2 \mathbf{I} \forall k$. All data-based approaches are trained on the same dataset \mathcal{H} .

Fig. 2 shows the MSE performance of the MFA-based channel estimator with $K = 64$ components in comparison with the baseline estimators introduced in Section IV-C (the GMM variants also have $K = 64$ components) for $T = 100,000$ (top) and $T = 10,000$ (bottom) training samples. We observe that the approaches ‘‘LS’’, ‘‘LMMSE’’, and ‘‘genie-OMP’’ as introduced in Section IV-C do not vary in the performance between both cases. The compressive sensing approach genie-OMP, although having genie knowledge of the sparsity order, does not perform well which indicates that the sparsity assumption in the DFT dictionary is too restrictive for the measurement data, cf. [18].

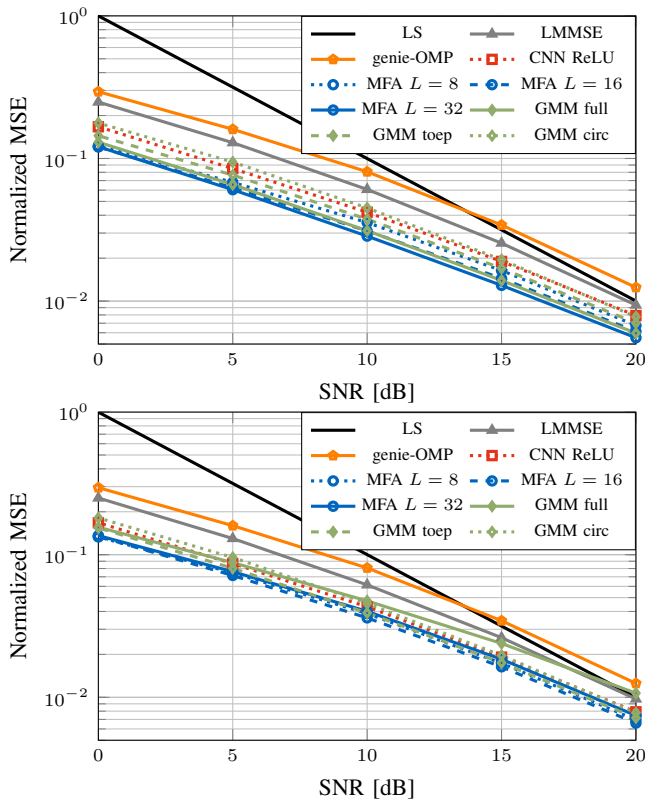


Fig. 2: MSE performance for $T = 100,000$ (top) and $T = 10,000$ (bottom) training samples for $K = 64$ components.

The CNN-based channel estimator, labelled “CNN ReLU”, cf. Section IV-C, performs better, but is almost always worse than the GMM- and MFA-based channel estimators, highlighting their strong performance.

For the case of $T = 100,000$ training samples in Fig. 2 (top), the GMM-based estimator with full covariances (“GMM full”) performs better than the Toeplitz (“GMM toep”) or circulant (“GMM circ”) structured versions, however, it is outperformed by the MFA-based estimator with $L = 32$ latent dimensions over the whole SNR range. Reducing the latent dimension further leads to a worse MSE, but the performance gap is small, especially in the low SNR regime, and the structured GMM variants are still outperformed for all SNRs.

In Fig. 2 (bottom), the case of $T = 10,000$ training samples is shown where the GMM-based estimator with full covariances suffers from overfitting, especially in the high SNR regime, cf. [6]. Although the structured GMM variants are less prone to overfitting, they are outperformed by the MFA-based estimator with $L = 8$ or $L = 16$ latent dimensions over the whole SNR range. Increasing the latent dimension to $L = 32$ leads to a slightly worse performance due to overfitting. Altogether, these results highlight the importance of the adaptive nature of the proposed MFA-based estimator, which allows to choose a suitable latent dimension for a limited amount of training data.

In Fig. 3, we further investigate the impact of the latent dimension L on the performance for $K = 64$ mixture components and for different numbers of training samples

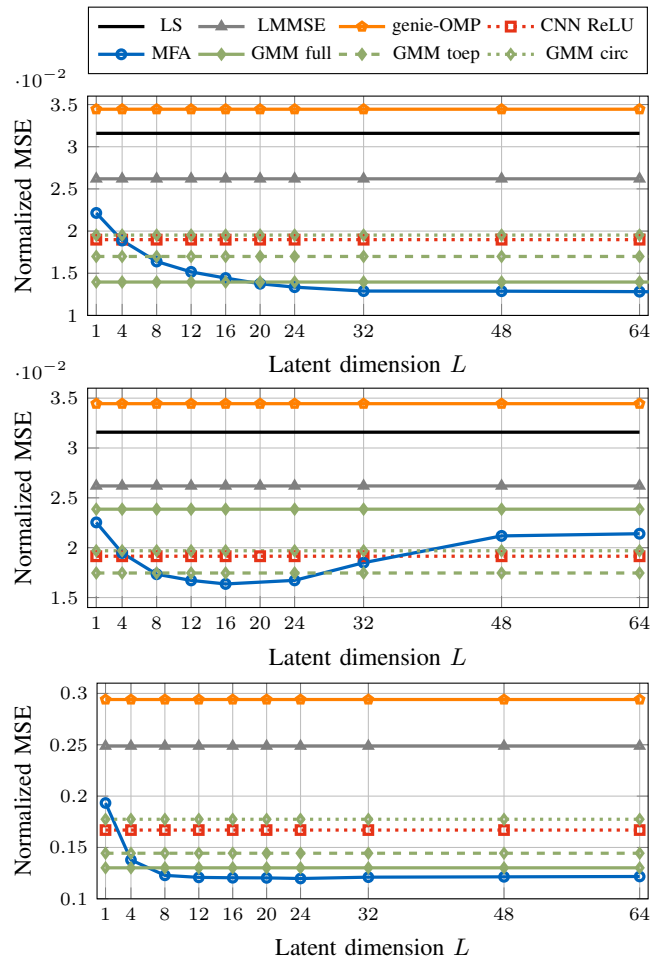


Fig. 3: MSE performance over the number L of latent dimensions for $K = 64$ components. Top: $T = 100,000$ and SNR = 15 dB. Middle: $T = 10,000$ and SNR = 15 dB. Bottom: $T = 100,000$ and SNR = 0 dB.

and SNR values. We compare the results with the baseline estimators which have a constant behavior with respect to the latent dimensions. In the top plot, the case of $T = 100,000$ and SNR = 15 dB is evaluated in which the MSE of the MFA-based estimator is consistently decreasing for higher latent dimensions, but with a saturation above $L = 32$. The approaches LS, LMMSE, and genie-OMP are outperformed already with a single latent dimension. All GMM-based variants and the CNN estimator are outperformed for $L = 20$ latent dimensions or more. The middle plot shows that for a small amount of training data $T = 10,000$ and SNR = 15 dB, the unstructured GMM-based estimator performs even worse than the MFA model with only a single latent dimension. Furthermore, increasing the latent dimension up to $L = 16$ yields a consistently better MSE performance, whereas a degradation can be observed for higher latent dimensions due to overfitting effects. In addition, even the structured GMM-based variants and the CNN estimator are outperformed for $L \in [8, 24]$ latent dimensions. In the bottom plot, a lower SNR value of 0 dB for $T = 100,000$ training samples is evaluated. The plot indicates that for lower SNR values, generally less latent dimensions are necessary since a

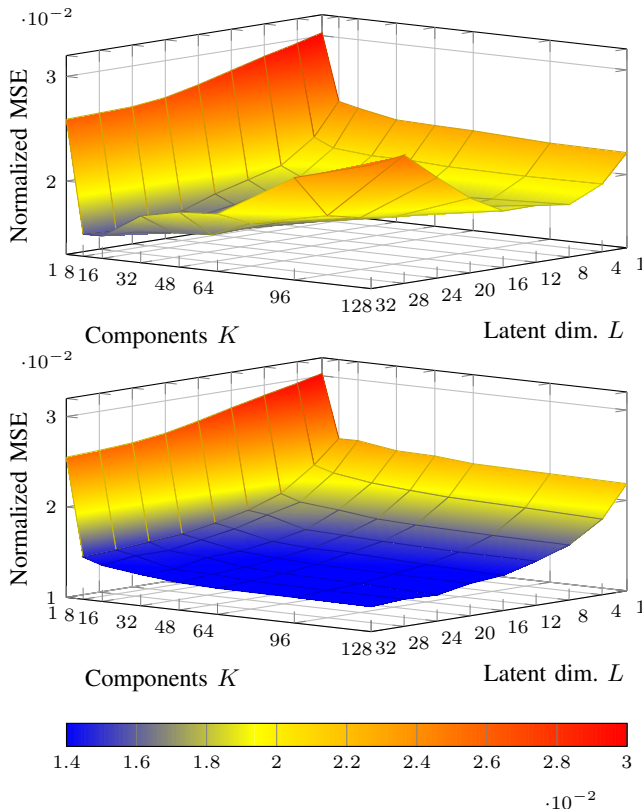


Fig. 4: MSE performance over the number of latent dimensions L and mixture components K for $T = 10,000$ (top) and $T = 100,000$ (bottom) training samples for an SNR of 15 dB.

saturation already occurs above $L = 12$. All baseline estimators are outperformed with $L = 8$ or more latent dimensions.

In Fig. 4, the combined impact of both the latent dimensions $L \in [1, 32]$ and mixture components $K \in [1, 128]$ on the MSE of the MFA model is shown for SNR = 15 dB. The case of $K = 1$ refers to the FA model as described in Section III. In the top plot for $T = 10,000$ it can be observed that the resulting MSE is minimal at $(K, L) = (8, 28)$ and it increases for higher numbers of latent dimensions and mixture components as expected due to overfitting. In contrast, for $T = 100,000$ training samples, the MSE is consistently decreasing for increasing latent dimensions and mixture components with an overall saturation effect. This analysis validates the asymptotic analysis up to a certain extent, since even if the latent dimension is fixed, the MSE can be further decreased by increasing the number of mixture components K . We note that this behavior inherently depends on the available amount of training data.

VI. CONCLUSION AND OUTLOOK

In this work, we have proposed to employ the MFA model for channel estimation which is asymptotically optimal in the sense that the convergence to the MSE-optimal CME is guaranteed. Thereby, the underlying (unknown) channel distribution of a whole communication scenario is learned offline by fitting the MFA parameters. Afterwards, the MFA model is leveraged for online channel estimation where especially the number of

parameters and computational complexity is reduced due to the inherent low-rank structure. Simulation results based on measurement data showed great estimation performances.

In future work, we plan to further investigate the MFA model for physical layer applications. Particularly interesting is to utilize the subspace information that is provided by the MFA, e.g., for interference channels, feedback applications [19], or in reconfigurable intelligent surface (RIS)-aided systems [20]. In addition, we want to adapt the approach to deal with imperfect training data and apply it to channels at higher frequencies.

REFERENCES

- [1] S. Roweis and Z. Ghahramani, "A Unifying Review of Linear Gaussian Models," *Neural Comput.*, vol. 11, no. 2, pp. 305–345, Feb. 1999.
- [2] T. T. Nguyen, H. D. Nguyen, F. Chamroukhi, and G. J. McLachlan, "Approximation by Finite Mixtures of Continuous Density Functions that Vanish at Infinity," *Cogent Math. Statist.*, vol. 7, no. 1, p. 1750861, 2020.
- [3] D. P. Kingma and M. Welling, "Auto-Encoding Variational Bayes," in *Proc. 2nd Int. Conf. Learn. Represent.*, 2014.
- [4] N. Shlezinger, J. Whang, Y. C. Eldar, and A. G. Dimakis, "Model-Based Deep Learning," *Proc. IEEE*, pp. 1–35, 2023.
- [5] M. Alsabab *et al.*, "6G Wireless Communications Networks: A Comprehensive Survey," *IEEE Access*, vol. 9, pp. 148 191–148 243, 2021.
- [6] M. Koller, B. Fesl, N. Turan, and W. Utschick, "An Asymptotically MSE-Optimal Estimator Based on Gaussian Mixture Models," *IEEE Trans. Signal Process.*, vol. 70, pp. 4109–4123, 2022.
- [7] M. Baur, B. Fesl, M. Koller, and W. Utschick, "Variational Autoencoder Leveraged MMSE Channel Estimation," in *56th Asilomar Conf. Signals, Syst., Comput.*, 2022, pp. 527–532.
- [8] B. Fesl, M. Joham, S. Hu, M. Koller, N. Turan, and W. Utschick, "Channel Estimation based on Gaussian Mixture Models with Structured Covariances," in *56th Asilomar Conf. Signals, Syst., Comput.*, 2022, pp. 533–537.
- [9] B. Fesl, N. Turan, M. Joham, and W. Utschick, "Learning a Gaussian Mixture Model from Imperfect Training Data for Robust Channel Estimation," *IEEE Wireless Commun. Lett.*, 2023.
- [10] K. P. Murphy, *Machine Learning: A Probabilistic Perspective*. The MIT Press, 2012.
- [11] Z. Ghahramani and G. E. Hinton, "The EM Algorithm for Mixtures of Factor Analyzers," University of Toronto, Tech. Rep., 1996.
- [12] Y. Tang, R. Salakhutdinov, and G. Hinton, "Deep Mixtures of Factor Analyzers," in *Proc. 29th Int. Conf. Mach. Learn.*, 2012, p. 1123–1130.
- [13] D. Ramírez, I. Santamaria, S. Van Vaerenbergh, and L. L. Scharf, "An Alternating Optimization Algorithm for Two-Channel Factor Analysis with Common and Uncommon Factors," in *52nd Asilomar Conf. Signals, Syst., Comput.*, 2018, pp. 1743–1747.
- [14] H. Xie, F. Gao, and S. Jin, "An Overview of Low-Rank Channel Estimation for Massive MIMO Systems," *IEEE Access*, vol. 4, pp. 7313–7321, 2016.
- [15] A. Alkhateeb, G. Leus, and R. W. Heath, "Compressed Sensing based Multi-User Millimeter Wave Systems: How Many Measurements are needed?" in *IEEE Int. Conf. Acoust., Speech, Signal Process. (ICASSP)*, 2015, pp. 2909–2913.
- [16] Y. C. Pati, R. Rezaifar, and P. S. Krishnaprasad, "Orthogonal Matching Pursuit: Recursive Function Approximation with Applications to Wavelet Decomposition," in *Proc. 27th Asilomar Conf. Signals, Syst., Comput.*, Nov. 1993, pp. 40–44 vol.1, ISSN: 1058-6393.
- [17] D. Neumann, T. Wiese, and W. Utschick, "Learning the MMSE Channel Estimator," *IEEE Trans. Signal Process.*, vol. 66, no. 11, pp. 2905–2917, Jun. 2018.
- [18] N. Turan, B. Fesl, M. Grundei, M. Koller, and W. Utschick, "Evaluation of a Gaussian Mixture Model-based Channel Estimator using Measurement Data," in *Int. Symp. Wireless Commun. Syst. (ISWCS)*, 2022.
- [19] N. Turan, B. Fesl, M. Koller, M. Joham, and W. Utschick, "A Versatile Low-Complexity Feedback Scheme for FDD Systems via Generative Modeling," 2023, arXiv preprint: 2304.14373.
- [20] B. Fesl, A. Faika, N. Turan, M. Joham, and W. Utschick, "Channel Estimation with Reduced Phase Allocations in RIS-Aided Systems," 2023, arXiv preprint: 2211.07552.